Using Brownian Dynamics to model nanoparticle aggregation under shear

Sergiy Markutsya, Shankar Subramaniam, Rodney O. Fox, and R. Dennis Vigil,
Iowa State University, Ames, IA

Introduction

Light-scattering data for the aggregation of colloidal nanoparticles shows that hybrid aggregates with two different fractal dimensions can be formed depending on the magnitude and duration of the applied shear (Mokhtari *et al*).[1] Formation of such super-aggregate structures with fracal dimension $D_f = 2.55$, and their reverting to $D_f = 1.8$ depending on the shear condition, is not completely explained yet. Simulations can provide insight into this behavior, provided they can accurately capture the essential aggregation physics. Brownian Dynamics (BD) simulations are used to study aggregation in this work. First, the numerical convergence requirements for BD simulations to study aggregation are established. These require that the computational time step be small enough to resolve three characteristic times: one corresponds to the frictional coefficient that is related to the dissipation of energy in the system, the second characteristic time is related to the shear force that applied to the system, and a third characteristic time corresponds to the systematic force that acts between nanoparticles. Statistics of nanoparticle aggregation such as cluster size distribution need to be estimated from the BD simulations. If BD of an equilibrium system is performed, then one can form estimates of such statistics using time-averaging once equilibrium is reached. For non-equilibrium, statistically time-evolving systems, time-averaging cannot be employed and ensemble averaging is needed. Since aggregation is a time-evolving process even in the statistical sense, multiple independent simulations (MIS) are needed to extract aggregation statistics for the BD simulations. In order to establish convergence of the BD results, numerical tests are performed to determine the time step and MIS required for accurate solution of simple system. Our tests reveal that even for such simple systems, a large number of MIS is needed to accurately estimate the probability of particles forming aggregates. Estimates for a system of N particles indicate the need for computational speed-up. Strategies to speed-up accurate BD calculations of aggregation are explored.

Simulation method

In a Brownian Dynamics simulation, the equations governing the evolution of a system of N monodispersed nanoparticles in a sheared liquid medium are

$$\begin{aligned} d\mathbf{r}_i &= \mathbf{v}_i dt \\ d\mathbf{v}_i &= -\gamma\left(\mathbf{v}_i - \mathbf{u}(\mathbf{r}_i)\right) dt + \frac{\mathbf{F}(\mathbf{r}_i)}{m} dt + \Sigma_v d\mathbf{W}_i, \quad i = 1, \ldots, N \end{aligned} \tag{1}$$

where $\mathbf{r}_i$ and $\mathbf{v}_i$ are the position and velocity of i^{th} nanoparticle respectively, and m is the mass of the nanoparticle. The first equation merely states that each nanoparticle's position evolves by its velocity. The second equation states that the velocity of a nanoparticle evolves under the action of (i) frictional drag arising from relative motion with liquid medium through the term $-\gamma\left(\mathbf{v}_i - \mathbf{u}(\mathbf{r_i})\right)$ (where γ is the friction coefficient), (ii) a systematic force $\mathbf{F}(\mathbf{r}_i)$ arising from interaction with other nanoparticles, and (iii) a random component $\Sigma_v d\mathbf{W}_i$ where $d\mathbf{W}_i$ is the increment of a Wiener process. In the frictional drag term, $\mathbf{u}(\mathbf{r}_i)$ is the fluid velocity at the nanoparticle location. (The solvent molecules in the fluid are not explicitly represented in the BD method.)

The systematic force $\mathbf{F}(\mathbf{r}_i)$ acting on the i^{th} nanoparticle arises due to the interaction with all other $N-1$ nanoparticles, and is obtained from a specified pair-potential. The coefficient of the Wiener process increment is specified such that $\Sigma_v^2 = 2\gamma\sigma_{v_\infty}^2$, where $\sigma_{v_\infty}^2 = k_B T/m$ is the velocity variance, k_B is the Boltzmann constant, and T is the reference temperature. In the limit of infinite dilution the nanoparticles do not interact and the systematic force is zero. This specification of Σ_v ensures that in the absence of a systematic force, the velocity variance evolves to a stationary value given by $\sigma_{v_\infty}^2$. The self-diffusion coefficient in the infinite dilution limit D_∞ is given by

$$D_\infty = \frac{k_B T}{m\gamma}. \tag{2}$$

When the liquid medium is sheared, the fluid velocity $\mathbf{u}_i^\alpha$ that is induced by the shear is given by

$$u_\alpha(\mathbf{r}) = G\delta_{\alpha 1}\delta_{\beta 2} r_\beta, \tag{3}$$

where G is the shear rate and r_β is the location of in tensor notation. An important nondimensional quantity that characterizes the ratio of the shear timescale to the diffusion timescale is is the Peclet number Pe, which is defined as

$$Pe = \frac{1}{4}\frac{G\sigma^2}{D_\infty}, \tag{4}$$

where D_∞ is the self-diffusion coefficient in the infinite dilution limit and σ is the particle diameter.

The systematic force $\mathbf{F}(\mathbf{r}_i)$ representing the interaction between nanoparticles is calculated as

$$\mathbf{F}(\mathbf{r}_i) = -\nabla_{\mathbf{r}_i} U \tag{5}$$

where U is a model pair-potential of interaction. In this work two potentials are used. The Lennard-Jones (LJ) potential, which is given by

$$U(r_{ij}) = 4\varepsilon\left[\left(\frac{r_{ij}}{\sigma}\right)^{12} - \left(\frac{r_{ij}}{\sigma}\right)^{6}\right] = 4\varepsilon\left[x^{12} - x^6\right] \tag{6}$$

where $x = r_{ij}/\sigma$, $r_{ij} = |\mathbf{r}_i - \mathbf{r}_j|$ is the distance between centers of the i^{th} and j^{th} particles, and ε is the well-depth. In the present work ε was chosen to be equal to $8k_B T$.

The DLVO potential consists of an electrostatic repulsion and a van der Waals attraction:

$$U(x) = J_0\frac{\exp[-k(x-1)]}{x} - \frac{A}{12}h(x) \tag{7}$$

where k is the reduced inverse Debye length, J_0 is the electrostatic coupling constant related to the surface, A is the Hamaker constant (is equal to $6.5\times 10^{-20}J$ for latex particles in water), and $h(x)$ describes the van der Waals attraction:

$$h(x) = \frac{1}{x^2-1} + \frac{1}{x^2} + 2\,ln\left(1 - \frac{1}{x^2}\right) \tag{8}$$

The parameters of DLVO potential where chosen in such way that the position of the second minimum is $x = 1.061$ with well depth $\varepsilon = 4k_B T$, and an energy barrier equal to $80k_B T$ at $x = 1.01$.

Temporal resolution of BD simulations

By reviewing velocity equation (1) we can distinguish three characteristic timescales which should be resolved. Those characteristic timescales are related to the frictional term, shear term, and timescale that is related to the systematic force. In order to get an accurate solution, the computational time step should be small enough to resolve all three timescales that are represented in this problem, which implies some restrictions.
Timescale τ_γ which is related to the frictional part can be represented as

$$\tau_\gamma = \frac{1}{\gamma} = \frac{D_\infty}{\sigma_{v_\infty}^2} \tag{9}$$

where D_∞ is the self-diffusion coefficient under an infinite dilution limit.
Timescale τ_s which is related to the shear part can be represented as

$$\tau_s = \frac{1}{G} = \frac{\sigma^2}{4PeD_\infty} \tag{10}$$

And the timescale τ_F which is related to the systematic force can be represented as

$$\tau_F = \frac{m\sigma\sigma_{v_\infty}}{\varepsilon} \tag{11}$$

By defining those characteristic timescales it is possible to determine the computational time step Δt. When modeling diffusion process with no shear by BD, timescale separation technique can be applied, as was shown by Giro *et al.*[2] In this case, three different algorithms of solving Langevin equation (1) can be used based on the timescale relations. When $\tau_\gamma \ll \Delta t \ll \tau_F$ an algorithm proposed by Ermak *et al.*[3] can be used. By applying this algorithm position and velocity Langevin equation (PVL) is reduced to the position Langevin equation (PL). If $\tau_\gamma \sim \Delta t \ll \tau_F$ an algorithm proposed by Allen[4] and Vangunsteren[5] can be used. In third case, when $\Delta t \ll \tau_F$ and $\Delta t \ll \tau_\gamma$ it is possible to use an algorithm proposed by Turq *et al.*[6] By modeling an aggregation process of latex nanoparticles in water for our choise of physical parameters all timescales have similar order of magnitude, such as $\tau_\gamma = 10.5$, $\tau_s = 0.25$, and $\tau_F = 0.125$ in reduced units σ/σ_{v_∞}. Thus, for aggregation we have to resolve all the timescales and the timescale separation does not exist. Based on this conclusion the computational time step Δt is needed to be chosen to be much smaller than a minimum value of those timescales. From the other hand the computational time step should be big enough for a reasonable running time. These limitations impose restrictions on such values as a Peclet number Pe and potential's well depth ε.

The right choice of the computational time step is a necessary but not sufficient condition to obtain an accurate computational result. Usually, some characteristic quantities should be analyzed in order to estimate how accurate an obtained solution is. From our previous work[7] we know that when using BD simulation to model an aggregation process, such characteristic quantities as Diffusivity and Radial Distribution Function (RDF) should be correctly described in order to get an accurate results.

As it was shown by Giro *et al.*[2], BD with Lennard-Jones potential is a valid method to model a diffusion process. However, at the same time the RDF is not described correctly. It was also shown that if interaction potential is changed to get a correct RDF (by replacing LJ potential with mean field potential (MF), the diffusivity data are going out of range. For the aggregation process

both diffusivity and RDF are important: diffusivity is related to the dynamics of the aggregates formation, and RDF is related to the structure of the aggregates, thus those parameters should be described correctly. A numerical experiment was set up to investigate this issue.[7]

In those work aggregation process was simulated by BD and Molecular Dynamics (MD) where MD was used as a reference system. For MD simulation a system with 1,354 solute particles (volume fractions $f_{v(solute)} = 0.0055$) and 148,753 solvent particles ($f_{v(solvent)} = 0.6$) which interact through LJ potential was used. Solvent and solute particles had the same size but different masses ($m_{solute}/m_{solvent} = 50$) and different potential's well depths ($\varepsilon_{solute}/\varepsilon_{solvent} = 4$). For BD simulation a system with 1,354 solute particles that interact throug the same LJ potential with well depth $\varepsilon_{solute}$was used. Such parameters as diffusivity and RDF were estimated for both MD and BD simulations. By comparing those parameters it was found that by modeling an aggregation process with MD and BD similar results for diffusivity and RDF were obtained. This fact brought us to the next conclusions: BD is a valid approach for calculating diffusion in far from the infinite dilution limit; getting simultaneously diffusion coefficient and RDF in correct way is critical for right description of the aggregation process.

Convergence of statistics

The multiple independent simulations (MIS) are needed to extract aggregation statistics. Therefore, to establish a convergence of BD simulations, a numerical test was performed to determine the time step and the number of MIS required for accurate solution of simple one-particle system. For this test a simple one dimensional system with one-particle was used. In this case the Langevin equation can be represented as:

$$\begin{aligned} dx &= v_x dt \\ dv_x &= -\gamma v_x dt + \frac{F(x)}{m} dt + \Sigma_v dW \end{aligned} \tag{12}$$

For the systematic force calculation a simple general ramp-well potential with two wells was used. Schematic plot of this potential is represented on Figure 1, and it is defined as

$$U(x) = \begin{cases} \infty, & 0 < x < \sigma \\ -\varepsilon \dfrac{x - x_a}{\sigma - x_a} - \varepsilon_2, & \sigma \le x \le x_a \\ -\varepsilon_2, & x_a \le x \le L \\ \infty, & x > L \end{cases} \tag{13}$$

where $x_a - \sigma$ is the width of the first well, $L - x_a$ is the width of the second well, and x_a is related to cut-off distance.
For such system, the PDF solution has a form[8,9]

$$P(x, v_x) = C_x P(x) C_{v_x} P(v_x) \tag{14}$$

where

$$P(x) = C_x \exp\left\{ -\frac{2\gamma}{m\Sigma_v^2} U(x) \right\} \tag{15}$$

$$P(v_x) = C_{v_x} \exp\left\{ -\frac{2\gamma}{m\Sigma_v^2} K(v_x) \right\} \tag{16}$$

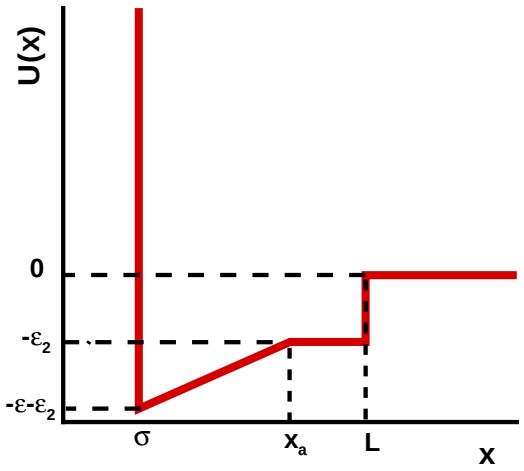

Figure 1: Schematic of general ramp-well potential for 1-D case

where $U(x)$ is the potential energy, and $K(v_x)$ is the kinetic energy.

Constants C_x and C_{p_x} can be found by integrating these equations over all values of x and v_x and applying those integrals to be equal to one:

$$\begin{aligned} C_{v_x} &= \sqrt{\frac{\gamma}{\pi}}\frac{1}{\Sigma_v} \\ C_x &= \left[\frac{\Sigma_v^2 m(\sigma - x_a)}{2\gamma\varepsilon}\left(1 - \exp\left\{\frac{2\gamma\varepsilon}{\Sigma_v^2 m}\right\}\right) + (L - x_a)\right]^{-1} \end{aligned} \tag{17}$$

In order to estimate the MIS number, it was defined the probability to have particle in the trapped state (particle lies in the interval $\sigma < x < x_a$), which is related to the probability of particles forming aggregates, where

$$\begin{aligned} p_a = p(\sigma < x \leq x_a) = \frac{\Sigma_v^2 m(\sigma - x_a)}{2\gamma\varepsilon}\left(1 - \exp\left\{\frac{2\gamma\varepsilon}{\Sigma_v^2 m}\right\}\right) \times \\ \left[\frac{\Sigma_v^2 m(\sigma - x_a)}{2\gamma\varepsilon}\left(1 - \exp\left\{\frac{2\gamma\varepsilon}{\Sigma_v^2 m}\right\}\right) + (L - x_a)\right]^{-1} \end{aligned} \tag{18}$$

After analytical definition of PDF solution, a set of numerical tests was performed to define the dependence of error on computational time step Δt and MIS number. For this purpose the system with such parameters is setting up: $\sigma = 1$, $m = 1$, $\varepsilon = 1$, $\gamma = 1$, $(x_a - \sigma) = 1$, $(L - x_a) = 0.6$, and $\sigma_{v_\infty}^2 = 1$. All the data are recorded at time $T_m = 10,000,000$ in reduced units $(\sigma/\sigma_{v_\infty})$.This set of parameters yelds the analytical value for the probability that particle will be in the trapped state as $p_a = 0.741$.

The compututional error can be defined as

$$e = \{p\}_{M,\Delta t} - p_a \tag{19}$$

where M is the number of MIS, and p_a is an analytical value for the probability to find particle in the trapped state. This error can be decomposed on the statistical error S_p and deterministic error

D_p as

$$e = \{p\}_{M,\Delta t} - p_a = [\{p\}_{M,\Delta t} - \langle\{p\}\rangle_{\Delta t}] + [\langle\{p\}\rangle_{\Delta t} - p_a] = S_p + D_p \tag{20}$$

where

$$S_p = \{p\}_{M,\Delta t} - \langle\{p\}\rangle_{\Delta t} \tag{21}$$

$$D_p = \langle\{p\}\rangle_{\Delta t} - p_a \tag{22}$$

where $\{p\}_{M,\Delta t}$ is the experimental data for the probability to find particle in the trapped state, and $\langle\{p\}\rangle_{\Delta t}$ is not known, but it can be estimated as

$$\langle\{p\}\rangle_{\Delta t} \approx p_{M_{max}}, \quad M_{max} = 10,000,000 \tag{23}$$

where M_{max} is the maximum number of MIS for the system.

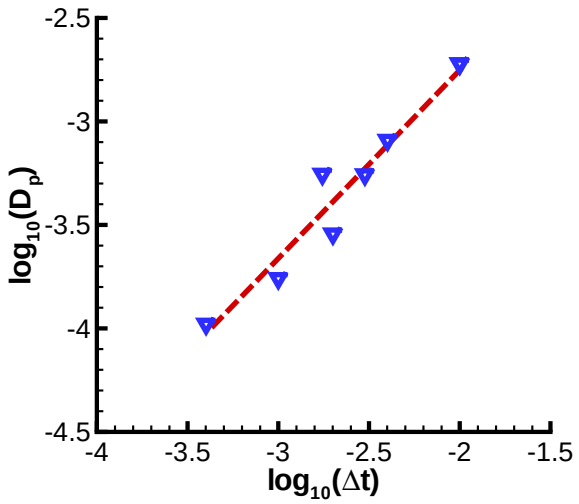

Figure 2: Deterministic error versus time step

Deterministic error was analyzed to define the dependence of error on computational time step Δt. It should depend on Δt as

$$D_p \sim \Delta t \tag{24}$$

The linear dependence between time step and deterministic error can be expected, because the deterministic error is defined as difference of first moments of p, and this is the case of the weak convergence. It was found that deterministic error D_p was decreased almost linearly (slope is equal to 0.92) with decreasing the time step Δt, as can be seen from the Figure 2.

Statistic error is analyzed to define the dependence of error on the number of MIS (M). Statistical error depends on M as

$$S_p = CM^{-1/2}\nu \tag{25}$$

where $\nu = N(0,1)$ is the normal distribution. Figure 2 represents the results of this test. From this figure we can determine that the slope is equal to -0.54 that is very close to the expected theoretical

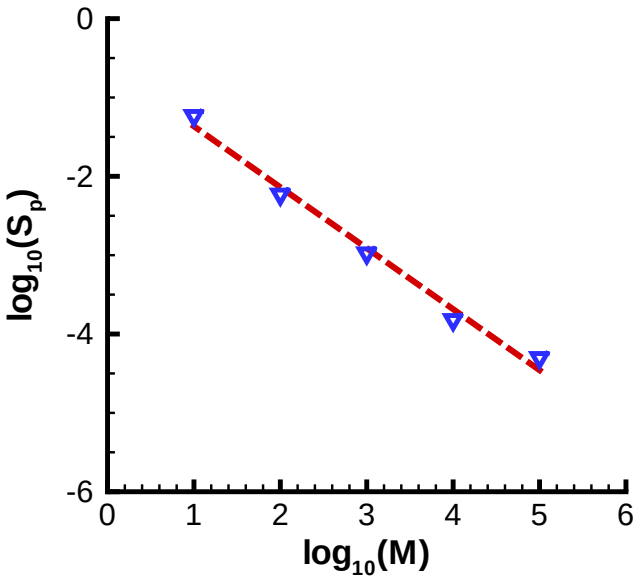

Figure 3: Statistic error versus the number of MIS M

value of -0.5. Based on the data represented in Figures 2 and 3 we can make a conclusion that results, obtained from those tests are consistent with the analytical results which validates the code.

The next question which we address is how many MIS are required to reduce statistical error S_p below a required tolerance level? To answer on this question the following computational experiment was performed. BD code for a single particle under the general ramp-well potential was running for a long time (from $T_m = 5,000$ to $T_m = 15,000$ with time step $\Delta t = 0.002$ in reduced

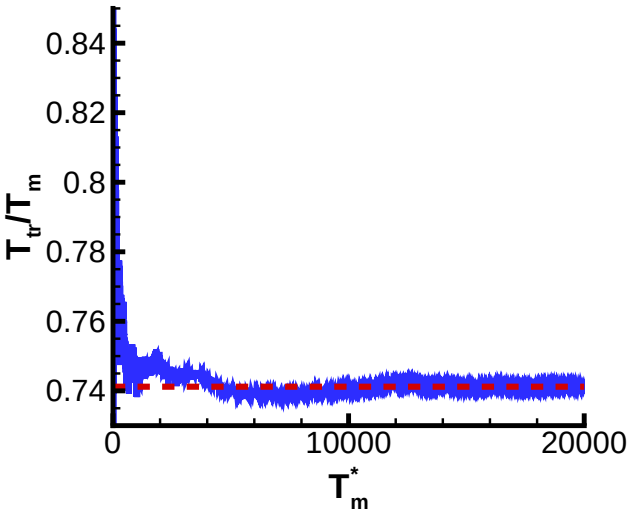

Figure 4: Ratio of the trapped time over the total time versus measurement time

units $(\sigma/\sigma_{v_\infty})$. The computitional estimate of p_a is given by T_{tr}/T_m, where T_{tr} is the total time

spent by particle in the trapped state, and T_m is the total measurement time. Dependence of this value on non-dimensional value $T_m^* = T_m\sigma_{v_\infty}/\sigma$ is shown on the Figure 4, where an analytical value is represented by dashed line. It is expected that value of this ratio will approach to the analytical value for the probability to find a particle in the trapped state p_a, calculated from (17). According to this plot the computed value closely approach the theoretical value only after $T_m^* = 5,000$ in reduced units σ/σ_{v_∞}. Based on this figure the number of MIS M is estimated by

$$M = \frac{T_m}{\langle T_{tr}\rangle} \tag{26}$$

where $\langle T_{tr}\rangle$ is the average time that particle spent in the trapped state which was calculated by running one-particle case for 1,000,000 times, or one run of 1,000,000 independent particles. Those results are represented in the Table 1.

As can be seen from the Table 1 more than 100 MIS are required to have an error value less that

Table 1. Expected MIS for the desired precision. Error is calculated as $e = |p_{tr} - p_a|/p_a$.

Error $e(\%)$	$p_{tr} = T_{tr}/T_m$	$\langle T_{tr}\rangle\sigma_{v_\infty}/\sigma$	M
10	0.8208	5.08	14.97
1.5	0.7522	4.51	116.19
0.5	0.7450	4.34	888.48
0.2	0.7397	4.29	2445.17
0.1	0.7420	4.32	2990.74

1.5% for one-particle case, and by requiring higher precision the number of MIS can easily reach up to several thousands. Thus, by increasing the number of particles in the system, the number of MIS will also increase by power law. This leads us to the conclusion that accurate estimation of aggregation formation for system of N particles requires a significant computational speed up.

Light Scattering analysis

Light scattering is the most frequently used tool for the analysis of aggregate structure.[10] For the system of N nanoparticles, the intensity of elastically scattered light can be represented as

$$I(\mathbf{q}) = NF(\mathbf{q})S(\mathbf{q}) \tag{27}$$

where $\mathbf{q}$ is the scattering wave vector, which is defined as

$$q = |\mathbf{q}| = \frac{4\pi}{\lambda}\sin(\theta/2) \tag{28}$$

where θ is the scattering angle, λ is the wavelength of light, $S(\mathbf{q})$ is the static structure factor, where

$$S(\mathbf{q}) = \frac{1}{N}\sum_k^N\sum_l^N \exp[i\mathbf{q}\cdot(\mathbf{r}_k - \mathbf{r}_l)] \tag{29}$$

Because nanoparticles are spherical particles of uniform density, then Eq.(8) can be reduced to

$$S(\mathbf{q}) = \frac{1}{N}\left|\sum_k^N \exp[i\mathbf{q}\cdot\mathbf{r}_k]\right|^2 = \frac{1}{N}\left|\sum_k^N[cos(\mathbf{q}\cdot\mathbf{r}_k) + i\ \sin(\mathbf{q}\cdot\mathbf{r}_k))]\right|^2 \tag{30}$$

and $F(\mathbf{q}) \rightarrow F(q)$ is the form factor for a sphere,

$$F(q) = \left[3\frac{\sin(qa) - qa\ \cos(qa)}{(qa)^3}\right]^2 \tag{31}$$

Because all modeled system are isotropic in cluster position and orientation it is valid to perform a spherical averaging by selecting over 200 different $\mathbf{q}$ values of constant magnitude, so $S(\mathbf{q}) \rightarrow S(q)$. This was done by creating the set of angles (θ, ϕ) according to a uniform differential solid angle $d\Omega$, and q is calculated from:

$$\mathbf{q} = |\mathbf{q}|(\sin(\theta)\cos(\phi)\mathbf{e}_1 + \sin(\theta)\sin(\phi)\mathbf{e}_2 + \cos(\theta)\mathbf{e}_3) \tag{32}$$

where $\mathbf{e}_i$ is the i^{th} Cartesian unit vector.

In case of a self-similar fractal aggregate with a fractal dimension D_f, $I(q)$ has the following three regimes: first regime is for small values of q (so called Rayleigh regime), where $I(q) = N$ the number of monomers per cluster. Second regime is for intermediate values of q, where $I(q) \sim q^{-D_f}$. And third regime is for very large q when Porod's law can be applied, so $I(q) \sim q^{-4}$. Analysis of modeled clusters with LS technique is a significant tool which can give such structure parameter like cluster's fractal dimension D_f. Comparison of this the fractal dimension with expected or measured values can give a good estimate of how accurate a BD simulation is.

Results and discussion

In this work the system of 108,882 monodispersed nanoparticles with diameter $\sigma = 2a = 3.4\ \dot{A}$ where a is the monomer radius, and box size $L = 117$ in monomer diameters are selected. The values for timescales are $\tau_\gamma = 10.5$, $\tau_s = 0.25$, and $\tau_F = 0.125$ in reduced units of σ/σ_{v_∞}. Based on those timescales the compututional time step is chosen to be $\Delta t = 0.0025$ in reduced units of σ/σ_{v_∞}. At least three MIS is runing to average all data for light scattering analysis.

In order to speed up calculation of the systematic force F, a cut-off distance r_c is introduced. In this case if the distance between particles is bigger than a cut-off distance $r > r_c$ the systematic force is equal to zero. Because, by introducing r_c we introduce some additional simplifications it is important to know how Light Scattering data depends on the value of cut-off distance. To answer this question BD code with implemented LJ potential is running two times with two different cut-off distances: $r_c = 3$ and $r_c = 5$ of monomer radius. On Figure 5 LS data obtained for those two cut-off distances is shown. The largest clusters have $N = 8900$ and $N = 8717$ for $r_c = 3$ and $r_c = 5$ correspondently and monomer volume fraction is $f_v = 0.035$. The positions of cut-off distances are marked by dashed line and labeled correspondently. According to Fry *et al.*[10] in the interval $a/R_{g,G} < qa < 2$ structure factor $S(q)$ should be $\sim q^{-D_f}$, where $D_f = 1.78$ is the fractal dimension, and $R_{g,G}$ is the ideal gel point radius of gyration defined as[10]

$$R_{g,G} = a\left[k_0^{-1}\left(\frac{D_f + 2}{D_f}\right)^{d/2} f_v\right]^{1/(D_f - d)} \tag{33}$$

where $k_0 \simeq 1.3$, and d is the space dimension. However, in our case $D_f \simeq 3.0$ for the range $(a/r_c < qa < 2)$ for both cut-off distances. Such behavior can be explained in the way that by implementing Lennard-Jones potential into BD the structure of the aggregate cannot be described correctly for the scale of potential's range. At the same time by setting up the cut-off distance

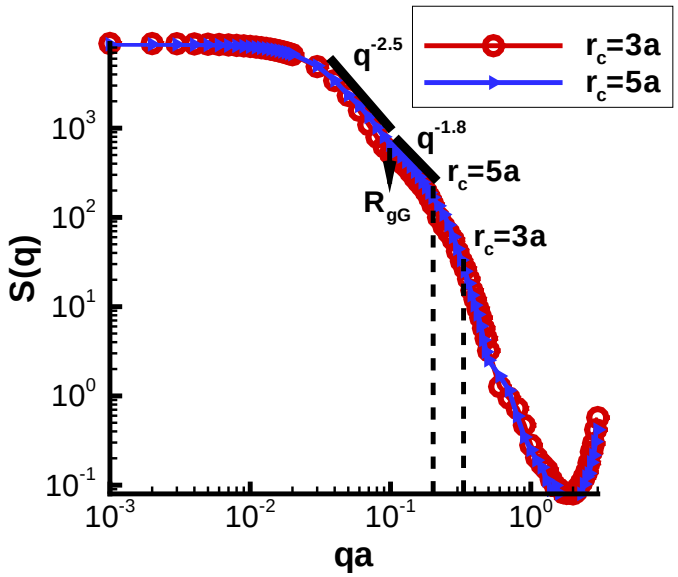

Figure 5: Structure of the largest cluster for 3-D BD simulation with LJ potential (with $r_c = 5.0a$ and $r_c = 3.0a$)

$r_c \to \infty$ the LS results should be similar to those obtained for $r_c = 5a$, because for LJ potential as $r > 5a$, the interaction potential $U \to 0$.

In the case of $r_c = 3a$ additional feature is observed. As can be seen from the Figure 5 in the range $a/R_{g,G} < qa < 0.2$, for both the curves $S(q) \sim q^{-1.8}$. Therefore it could be reasonable to expect that for case with cut-off distance $r_c = 3a$ in the range $0.2 < qa < 0.33$ there will be the same slope. But in fact this slope is different. This anomalous behavior should be investigated more precisely, but the most reasonable explanation of this phenomena lies in the presence of the local structure with the length scale of $l_s \simeq 5a$ and its nature can be similar to that discovered by Oh *et al.*[11] When $qa < a/R_{g,G}$ the slope of two curves is identical and defines $D_f = 2.5$. This is very rough approximation because of the narrow range for qa which caused by small size of the system. Increasing of the system size significantly increases the computational time that is required some steps to speed up BD calculations.

An influence of different potentials of interaction on the shape of LS data is also investigated. For this purposes LJ and DLVO potentials are chosen. It should be pointed out that DLVO potential is very "sticky", so when particle gets to an aggregate there is a very small probability that it will leave this aggregate, while for the LJ potential there is a higher possibility for particle to escape from an aggregate. Figure 6 represents LS data for two largest aggregates modeled with BD by implementing LJ and DLVO pair potentials with cut-off distance $r_c = 3.0a$ for both potentials with number of monomer in aggregate $N = 28000$ and $N = 32000$ for LJ and DLVO potentials correspondently.

As can be seen from this plot, LS analysis gives different shapes of structure factor spectra. This difference can be explained by presence of the anomalous area for the LJ potential in the range $0.2 < qa < 0.33$, discussed above. At the same time the slopes for both potentials have similar values for $qa < 0.2$ that allows us to make a conclusion that structure of aggregates modeled by BD for $DLVO$ and LJ potentials is similar for both potentials.

To investigate an influence of the shear onto the aggregation process a small shear is applied to the system ($Pe = 3.5 \times 10^{-2}$). In 3-D system shear was applied into the one Cartesian coordinate

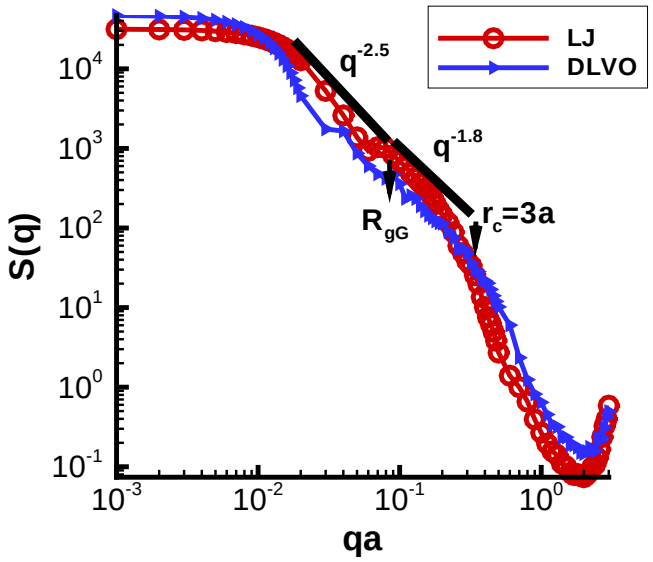

Figure 6: Structure of the largest cluster for 3-D BD simulation with LJ and DLVO potentials

only with zero shear at the middle of the system. In such case the system has two opposite velocity gradients induced by shear (like liquid between two disks which are spinning in opposite directions). From the previous work[1] it is known that when an aggregating system is exposed to the shear for some initial time and then shear released there are three different system's behaviors are observed depending on the strength of the shear. In case of low shear rate ($Pe < 1.0$), the aggregates will have essentially the same structure as without shear, with fractal dimension close to 1.7, however it will require less time to reach the gelling state. By increasing the shear rate, system behavior changing in such a way that immediately after releasing a shear in addition to the first slope that corresponds to $D_f = 1.7$ a second slope appears that corresponds to $D_f = 2.5$. However, further Brownian aggregation changes this double structure, and by reaching the gelling state the only one slope which is related to $D_f = 1.7$ is observed. When very high shear rate is applied, again, after releasing a shear an additional slope occurs, but it is not vanished even when reaching the gelling state.

The results of LS data for BD simulations for system with and without shear are represented on Figure 7 for LJ potential. LS analysis shows a good matching of data for shear and non-shear case for similar sizes of aggregates. A similar results where obtained for $DLVO$ potential. It should be pointed out that by applying shear to the system in order to have a similar size of an aggregate it is required only $20 - 25\%$ of time by comparing with a system with no shear. Those data represent that BD simulation for system with low shear rate describes the system behavior in expected way by comparing with the experimental results.

The next logical step will be to model an aggregation process under medium and high shear rate by using BD simulation. The further increasing of the shear rate (increasing of Pe number) requires decreasing of the computational time step Δt, therefore a significant speeding up of the BD code is required.

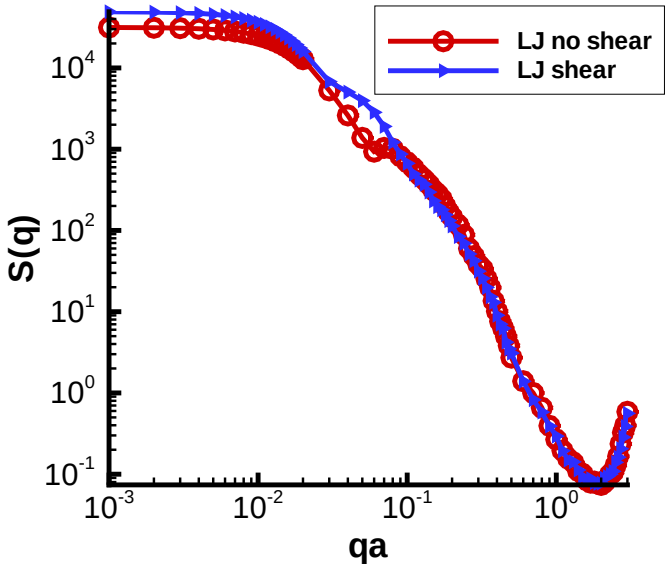

Figure 7: Effect of shear on the structure factor *S(q)* for BD with LJ potential

Conclusions

The Brownian Dynamics simulation method is investigated with the objective of determing if it is an appropriate approach to model aggregation with and without shear. When modeling aggregation with BD simulation all timescales have to be resolved with no timescale separation possible. An estimate of the number of Multiple Independent Simulation shows that a high number of MIS ($M > 100$) is required for one-particle system to reach a precision of 1.5% which makes this method to be very expensive in terms of computational time for system with N particles. Light scattering analysis can be successfully used to determine aggregate structure, however it requires to have a large system with $N \sim 800,000$, therefore some steps should be perform to speed up BD code. Light Scattering analysis shows that BD approach describes the structure of aggregates in predicted way for the range $qa < 0.2$. In case of a small shear rate BD approach models an aggregation dynamics in an appropriate and expected way.

We propose several strategies to speed up BD code: decrease a cut-off distance to $r_c = 4.0a$, and to parallelize the BD code and get significant speed up by running code on multiple processors.

References

1. T. Mokhtari, C.M. Sorensen, and A. Chakrabarti (unpublished).
2. A. Giro, E. Guardia, and J.A. Padro, Molecular Physics, **55**, 1063, 1985.
3. D.L. Ermak, and J.A. McCammon, Journal of Chemical Physics, **69**, 1352, 1978.
4. M.P. Allen, Molecular Physics, **40**, 1073, (1980).
5. W.F. Van Gunsteren, and H.J.C. Berendsen, Molecular Physics, **45**, 637, (1982).
6. P. Turq, F. Lantelme, and H.L. Friedman, Journal of Chemical Physics, **66**, 3039, 1977.
7. S. Markutsya, S. Subramaniam, M. Lamm, D. Vigil, R. Fox, *Assessing the applicability of Brownian Dynamics to simulation of nanoparticle clustering in liquid suspensions*, Proceedings of the 58^{th} Annual Meeting of the Division of Fluid Dynamics, Vol.50, No.9, November 2005.
8. V.I. Klyatskin, *Stochastic Equations Through the Eye of the Physicist: Basic concepts, Exact*

Results and Asymptotic Approximations, Boston, 2005.
9. C.W. Gardiner, *Handbook of stochastic methods: for physics, chemistry, and the natural sciences*, New York, 2004.
10. D. Fry, A. Chakrabarti, W. Kim, and C.M. Sorensen, Physical Review E **69**, 061401, 2004.
11. C. Oh, and C.M. Sorensen, Physical Review W **57**, 784, 1998.